Nuclear transit of human zipcode-binding protein IMP1

Jacob NIELSEN*, Sidsel K. ADOLPH*, Ewa RAJPERT-DE MEYTS†, Jens LYKKE-ANDERSEN*[1], Grete KOCH‡, Jan CHRISTIANSEN* and Finn C. NIELSEN‡[2]

*Institute of Molecular Biology, University of Copenhagen, Copenhagen, Denmark, †Department of Growth and Reproduction, Rigshospitalet, Blegdamsvej 9, DK-2100 Copenhagen, Denmark, and ‡Department of Clinical Biochemistry, Rigshospitalet, Blegdamsvej 9, DK-2100 Copenhagen, Denmark

The human IMPs (insulin-like growth factor II mRNA-binding proteins) belong to a vertebrate zipcode-binding protein family consisting of two RNA recognition motifs and four K homology domains and have been implicated in cytoplasmic mRNA localization, turnover and translational control. In the present study, we show that IMP1 is capable of translocating into nuclei of NIH 3T3 fibroblasts and its immunoreactivity is present in the nuclei of human spermatogenic cells. IMP1 does not contain a simple import signal, but nuclear entry was facilitated by disruption of RNA binding and cytoplasmic granule formation. IMP1 contains two NESs (nuclear export signals) within the RNA-binding K homology domains 2 and 4. The former is a leucine-rich leptomycin B-sensitive NES, whereas the latter is a leptomycin B-insensitive NES. Taken together, these results indicate that IMP1 may attach to its target mRNAs in the nucleus and thereby define the cytoplasmic fate of the transcripts.

Key words: K homology domain, mRNA export, NES (nuclear export signal), RNA-binding protein.

INTRODUCTION

The ZBPs (zipcode-binding proteins) such as ZBP1 (chicken), Vg1RBP/VERA (Vg1 RNA-binding protein/VgLE binding and endoplasmic reticulum association; *Xenopus*), CRD-BP (mouse) and IMP (insulin-like growth factor II mRNA-binding protein)/KOC (human) are orthologous and paralogous members of the same vertebrate RBP (RNA-binding protein) family, consisting of two RRMs (RNA recognition motifs) and four KH (K homology) domains (see [1], where the authors suggested the acronym VICKZ for this protein family). The KH domains are phylogenetically conserved in invertebrate homologues such as *Drosophila melanogaster* and *Caenorhabditis elegans*, and constitute a functionally independent entity [2]. The invertebrates contain a single member of this gene family whereas the examined vertebrates, with the apparent exception of *Xenopus*, have three members [3]. So far, only a handful of mRNA targets have been identified, and *cis*-elements occur in 5′-untranslated, coding or 3′-untranslated regions (UTRs). With the exception of the original zipcode identified in β-actin 3′-UTR, the elements appear to be relatively large (>100 nt) and unstructured. The proteins are expressed during early embryogenesis and at mid-gestation in the mouse [4]. They have also been implicated in post-transcriptional processes such as mRNA localization, turnover and translational control [5]. IMP and other members of the family have been detected only in the cytoplasm, but the presence of both putative import and export signals indicate that they could function as nucleocytoplasmic shuttling proteins, possibly influencing pre-mRNA processing and mRNA export [6,7]. Moreover, IMP3 has been identified as a member of the HeLa spliceosome [8], and the chicken homologue ZBP1 has recently been shown to be targeted to pre-mRNA transcripts by high-speed imaging [9].

Proteins smaller than approx. 50 kDa can diffuse passively through the NPC (nuclear pore complex), whereas the facilitated transport of larger proteins depends on transport signals such as NES (nuclear export signal), NLS (nuclear localization signal) or bi-directional shuttling signal [10,11]. The transport signals interact either directly or indirectly via adaptors, with transport receptors that mediate passage through the NPC. A majority of examples described for protein export was performed by the CRM1/exportin1 receptor, which belongs to the importin β-superfamily. It functions via three types of interactions, namely binding to the cargo, interaction with nucleoporins in the NPC and interaction with the GTPase Ran, which defines the directionality of transport. The integrity of the export complex is sensitive to the drug leptomycin B. Many RBPs have been shown to shuttle. Although the majority is predominantly nuclear at steady state, it has been proposed that mRNAs are exported via co-transcriptional association with shuttling hnRNPs (heterogeneous nuclear ribonucleoproteins) such as hnRNP A1 [12].

In the present study, we show that IMP1 is capable of translocating into the nucleus and contains NESs within the RNA-binding KH2 and KH4 domains. The former is a predicted leptomycin B-sensitive leucine-rich NES, whereas the latter is a novel and conserved leptomycin B-insensitive NES. Taken together, these results indicate that IMP1 may attach to its target mRNAs in the nucleus and thereby define the cytoplasmic fate of the transcripts.

MATERIALS AND METHODS

Generation of DNA constructs and recombinant proteins

GFP (green fluorescent protein)–IMP1 expression vector for transient transfections was generated by inserting the open reading frame of human IMP1 into the *Bgl*II and *Eco*RI sites of the pEGFP-C1 vector (ClonTech, Palo Alto, CA, U.S.A.). For stable

Abbreviations used: FRAP, fluorescence recovery after photobleaching; GFP, green fluorescent protein; hnRNP, heterogeneous nuclear ribonucleoprotein; IMP, insulin-like growth factor II mRNA-binding protein; KH, K homology; NES, nuclear export signal; NF90, nuclear factor 90; NLS, nuclear localization signal; NPC, nuclear pore complex; RBP, RNA-binding protein; RRM, RNA recognition motif; RT, reverse transcriptase; SV 40, Simian virus 40; TBS, Tris-buffered saline; UTR, untranslated region; YFP, yellow fluorescent protein; ZBP, zipcode-binding protein; for brevity, the one-letter system for amino acids has been used: L318, e.g. means Leu^{318}.

[1] Present address: Molecular Cellular and Developmental Biology, University of Colorado, CB 347, Boulder, CO 80309-0347, U.S.A.

[2] To whom correspondence should be addressed (e-mail FCN@rh.dk).

expression, GFP–IMP1 was inserted into the pBABE retroviral vector [13]. Briefly, GFP–IMP1 was excised from pEGFP-C1 and cloned into the *Xba*I site of pGEM11. The fragment was subsequently excised with *Bam*HI and *Eco*RI and inserted into the *Bam*HI and *Eco*RI sites of pBABE puro. IMP1 deletion mutants were generated by PCR with primers containing *Eco*RI (forward primers) and *Bam*HI (reverse primers) sites. The fragments were cloned into the *Eco*RI and *Bam*HI sites of pEGFP-C2. pHM 840 and pHM 830, encoding GFP–β-galactosidase with or without the SV 40 (Simian virus 40) NLS, respectively were kindly provided by T. Stamminger [14]. GFP-KH4-TCP80/NF90 (where NF90 stands for nuclear factor 90) was generated from a GFP–KH4 construct by insertion of full-length TCP80/NF90 downstream of KH4. Human H19[1–1603] (H19C) was inserted into an intronless version of pcDNA1 [15]. In H19C-IGF-IIsegC (where IGF stands for insulin-like growth factor) and H19C-A11, the high-affinity IMP1-binding sites from IGF-II leader 3 segment C [4] and A11 were cloned into pcDNA1-H19C respectively. A11 was obtained by a cDNA-SELEX experiment essentially as described in [16]. A11 contains one IMP1 attachment site with an apparent K_d of 0.2 nM and corresponds to nt 760–892 in the mouse IGF-II 3′-UTR.

Site-directed mutagenesis

Site-directed mutagenesis was performed with the QuikChange® kit (Stratagene, La Jolla, CA, U.S.A.) according to the manufacturer's instructions. Mutations in the KH4 NES were generated using GFP–IMP1[485–527] as template, and all these mutations resulted in alanine substitutions. Mutations in full-length GFP–IMP1 were V486A, EE484–485AL, EEV484–486AAA, VKL486–488AAA and HIR491–493AAA. The GXXG mutant with a 50-fold decreased RNA-binding affinity was obtained by inserting EL for XX in the signature loop of KH1, KH2 and KH3.

Cell culture, transfections and imaging

Mouse NIH 3T3 embryo fibroblast cells were obtained from the A.T.C.C. and routinely maintained in RPMI 1640 medium, supplemented with 10 % (v/v) foetal calf serum or in Dulbecco's modified Eagle's medium containing 10 % foetal calf serum. Stable GFP–IMP1 expressing NIH 3T3 cells were generated by retrovirus-mediated insertion of the pBABE-GFP-IMP1 as described in [13]. Transient transfections were performed with LIPOFECTAMINE™ 2000 (Life Technologies, Gaithersburg, MD, U.S.A.) according to the manufacturer's instructions. Briefly, 30 000 cells/cm^2 were seeded on glass plates 24 h before transfection. Cells were transfected with 2 μg/ml of the relevant plasmid and left for 24–48 h before the GFP-fusion proteins were examined with a confocal Zeiss LSM510 microscope.

Immunohistochemistry

Samples of human testicular tissues were obtained during orchidectomy of patients with testicular tumours for diagnostic purposes (the use of tissue samples for research after completed pathological assessment was approved by the local Ethics Committee). The tissue specimens used in the present study were either snap-frozen and stored at -80 °C, or fixed in Stieve's fluid or formalin, paraffin-embedded and stored at 4 °C. Staining with anti-IMP1 polyclonal rabbit antiserum, which exhibits some cross-reactivity towards IMP3 [4] or with anti-IMP3 antiserum, was performed by a standard indirect immunoperoxidase method, as described previously [17]. Briefly, frozen tissue sections were air-dried and fixed in Stieve's fluid, formalin or acetone, whereas paraffin-embedded sections were deparaffinized and re-hydrated. After washing in TBS (Tris-buffered saline, pH 7.6), all sections were incubated in 3 % H_2O_2 to quench the endogenous peroxidase activity. Subsequently, the sections were coated with diluted goat serum to block unspecific binding sites and incubated overnight with the primary antiserum at 4 °C. For negative controls, the specific antiserum was substituted with diluted non-immune rabbit serum (Dako, Glostrup, Denmark). The remaining procedure was performed at room temperature (20 °C). After three washes with TBS, sections were incubated for 30 min with a biotinylated goat-anti-rabbit IgG (Zymed, San Francisco, CA, U.S.A.), washed with TBS and incubated with peroxidase-conjugated streptavidin (Zymed) for 30 min. After a final rinse with TBS, sections were incubated with the peroxidase substrate aminoethyl carbazole (Dako) for 10 min, resulting in a red staining. Finally, some sections were lightly counterstained for 1 s in Mayer's haematoxylin to visualize unstained nuclei.

Western-blot analysis

Western-blot analysis was performed as described in [4]. Briefly, frozen tissues (approx. 100 mg) were crushed and resuspended in 2 × SDS/polyacrylamide load buffer. Proteins were separated on 10 % (w/v) SDS/polyacrylamide gels and transferred to Hybond-P membranes (Amersham Biosciences). After blocking, membranes were incubated overnight with anti-IMP1 or anti-IMP3 antibody in blocking solution at 4 °C and with horseradish peroxidase-conjugated anti-rabbit IgG for 1 h at room temperature. Immunoreactive proteins were detected with Supersignal reagents according to the manufacturer's instructions (Pierce).

RT (reverse transcriptase)–PCR

IMP1 and IMP3 mRNA expressions were determined by SYBR-green-based real-time RT–PCR, according to the manufacturer's instructions (Roche, Rotkreuz, Switzerland). Briefly, 1 μg of total RNA from human testis, liver or heart was reverse-transcribed by AMV (avian-myeloblastasis-virus) RT and random hexamers at 42 °C in a 15 μl reaction. The cDNA reaction mixture (1 μl) was used in the subsequent PCR. IMP1 cDNA was amplified by 30 cycles of PCR with primers hIMP1 567F, CAAGCAGCAGCAAGTGGACA (sense), and hIMP1 745R, TGGAGTGCACACTGATGGCT (antisense) and IMP3 cDNA was amplified with primers hIMP3 1010F, CCAAAGCTGAGGAGGAGATC (sense), and hIMP3 1224R, GGAGGAGTCATGGCTGAAAG (antisense). Moreover, β-actin cDNA was amplified with primers hβ-actin-51F, TCCTGTGGCATCCACGAAAC, and hβ-actin-31R, GAAGCATTTGCGGTGGACGAT, for control of the cDNA. All primer sets were placed in different exons to distinguish between amplification of genomic DNA and cDNA.

RESULTS

Nuclear localization of IMP1

Previous stainings of tissues and cultured cells have demonstrated that IMP proteins are mainly cytoplasmic at steady state [4]. A fusion between GFP and IMP1 (GFP–IMP1), stably expressed in

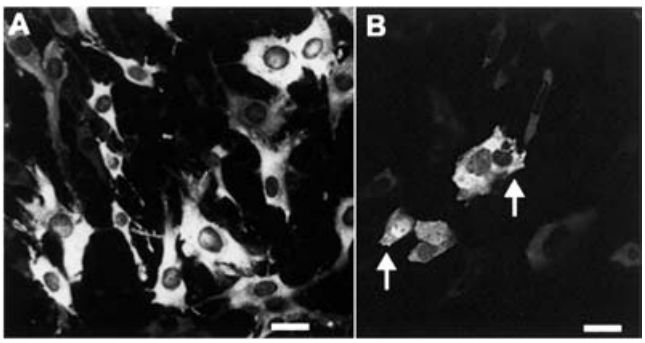

Figure 1 Nucleocytoplasmic distribution of GFP–IMP1

(**A**) NIH 3T3 cells stably expressing GFP–IMP1 under the control of Moloney leukaemia virus long-terminal repeat promoter [13]. The expression level of GFP–IMP1 is about twice as high as the relatively low endogenous level of IMP1 in NIH 3T3 cells, and GFP–IMP1 behaves like the endogenous IMP1 in terms of RNA binding, subcytoplasmic localization and sedimentation behaviour [2]. Scale bar, 25 μm. (**B**) NIH 3T3 cells transiently transfected with GFP–IMP1 under control of the CMV promoter. The expression level in these cells is between three and 20 times higher than the endogenous level: 15–20 % of the cells exhibit some degree of nuclear GFP–IMP1 staining, cells with and without GFP–IMP1 in the nucleus are marked with arrows. Other tested proteins (actin, tubulin or β-galactosidase) show the expected cytoplasmic distribution in the cells that exhibit GFP–IMP1 in the nucleus (results not shown). Scale bar, 22 μm.

NIH 3T3 cells at levels 2-fold above the relatively low concentration of endogenous IMP [2], is also predominantly cytoplasmic at steady state (Figure 1A). However, after transient expression of high levels of GFP–IMP1, we find that it accumulates in the nucleus. The GFP–IMP1 cDNA was under the control of a CMV promotor that resulted in a 3–20-fold higher expression than the endogenous level. The presence of GFP–IMP1 in the nucleus was observed in 15–20 % of the transfected cells (Figure 1B), and was mainly seen in strongly expressing cells, although not all strongly expressing cells exhibited nuclear accumulation. Nuclear IMP1 was excluded from the nucleolus, but otherwise the nuclear appearance did not exhibit signs of compartmentalization.

To identify a 'physiological' correlation to the nuclear accumulation in NIH 3T3 cells, we examined the subcellular distribution of IMP1/IMP3 immunoreactivity in a series of foetal and adult tissues from mouse and human. As described previously, a vast majority of immunopositive tissues exhibited cytoplasmic staining, but adult human testis showed IMP1/IMP3 immunohistochemical reactivity in nuclei of spermatogenic cells (Figure 2A). In contrast, cytoplasmic staining was observed in malignant germ cells and in germ-cell-derived tumours with an embryonic phenotype such as embryonal carcinoma (Figure 2Ad). An RT–PCR analysis (Figure 2B) and a Western-blot analysis (Figure 2C) of various tissue types, including human testis, revealed the presence of IMP1 mRNA and IMP1/IMP3 immunoreactivity of the expected size respectively.

The conditional nuclear accumulation of IMP1 suggests that IMP1 can be both imported and exported from the nucleus. Therefore import of GFP–IMP1 into the nucleus was examined by FRAP (fluorescence recovery after photobleaching). NIH 3T3 nuclei, exhibiting moderate nuclear accumulation of GFP–IMP1, were photobleached and monitored by time-lapse microscopy (Figure 3). After 25 min, half-maximal recovery was obtained, and full equilibration was observed within an hour. GFP–β-galactosidase and GFP–β-galactosidase with NLS from SV 40 large-T antigen were included as negative and positive controls respectively (Figure 3).

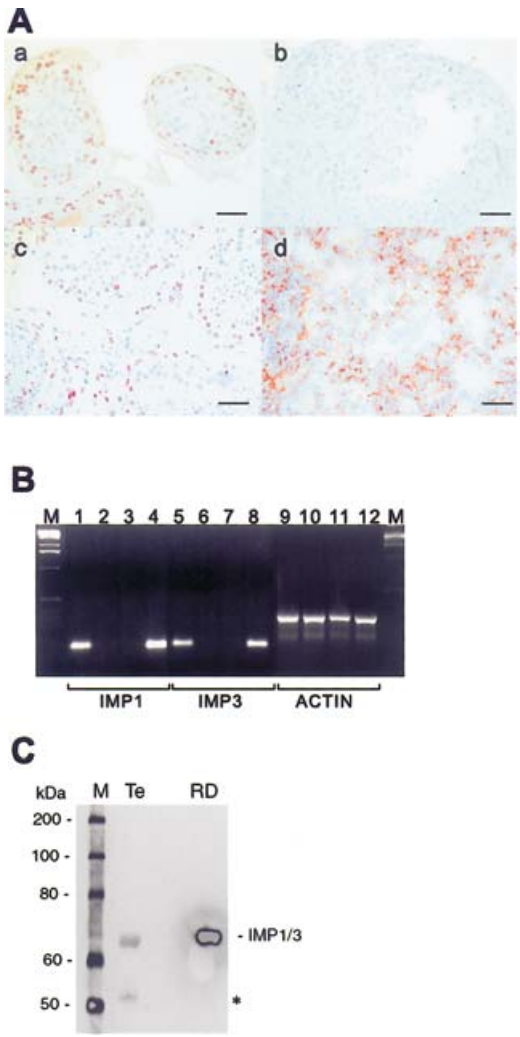

Figure 2 Nucleocytoplasmic distribution of IMP1/IMP3 immunoreactivity in human testis

(**A**) Human testis stained with anti-IMP1 antibody (**a**), anti-IMP3 antibody (**c**) or a negative control with the primary antibody replaced by preimmune rabbit serum (**b**) and counterstained with haematoxylin; scale bars, 40 μm. The IMP-positive nuclei are stained red. (**d**) Cytoplasmic distribution of IMP1 immunoreactivity in a testicular embryonal carcinoma; scale bar, 25 μm. (**B**) RT–PCR analysis of IMP1 (lanes 1–4) and IMP3 (lanes 5–8) mRNA expression in human testis (lanes 1 and 5), liver (lanes 2 and 6), heart (lanes 3 and 7) and rhabdomyosarcoma cells (lanes 4 and 8) that express IMP1 and IMP3 [4]. Lanes 9–12 show the amplification of β-actin cDNA for control purposes. (**C**) Western-blot analysis of IMP1/IMP3 immunoreactivity in human testis. M, marker; Te, testis; RD, rhabdomyosarcoma cells. *A minor band in testis that may represent a proteolytic cleavage product.

Apparent lack of a simple import signal

Inspection of the sequence of the mouse and chicken orthologues had previously led to the suggestion that amino acids between RRM1 and RRM2 and between RRM2 and KH1 constitute putative NLSs [6,7]. We examined the NLS activity of the equivalent human peptides by inserting them between GFP and β-galactosidase into the pHM 830 vector [14]. Neither KKQRSRK nor QNGRRG was capable of conferring import of the chimaeric protein (results not shown). To broaden the search, the entire IMP1 protein was divided into three segments on the basis of the positions of the two NESs (see below), and each of these segments was examined for the presence of an import signal by insertion into the pHM 830 vector (Figure 4). The previously

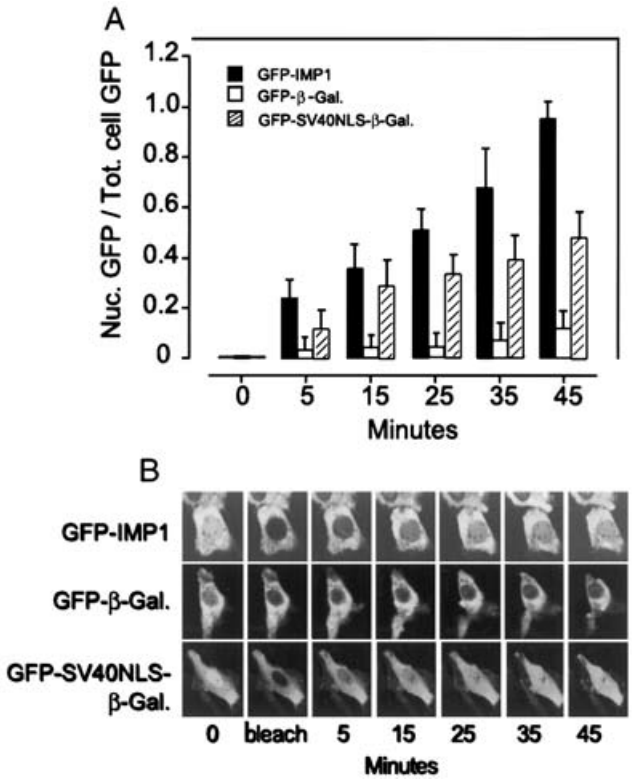

Figure 3 FRAP analysis of GFP–IMP1 import and time-lapse microscopy of an NIH 3T3 cell with moderate nuclear accumulation

(**A**) Bars represent the relative nuclear staining at different times after bleaching compared with the relative nuclear staining before bleaching; relative intensity of staining immediately before bleaching is set to 1 and the relative staining after bleaching is set to 0. The results are means $\pm$ S.D. from three separate experiments. (**B**) A representative set of frames used to obtain the graph in (**A**). The nucleus was photobleached at t_0, and subsequently pictures were taken after 5 min and then every 10 min. Within 25 min, the relative level of GFP–IMP1 in the nucleus was half of the level it was before bleaching, and equilibration was achieved after approx. 1 h. The kinetics of equilibration was not significantly different between cells with low or high nuclear accumulation. Cells transfected with GFP–β-galactosidase were used as a negative control and the positive control encompasses the NLS from SV 40 large-T antigen. GFP–β-galactosidase contains no nuclear transport signals and due to its large size, it is not expected to traverse the nuclear membrane to any considerable extent. As expected, GFP–β-galactosidase exhibited exclusively cytoplasmic staining in approx. 95% of the cells, but in the cells where some GFP–β-galactosidase had entered the nucleus, there was no significant equilibration after bleaching.

characterized NLS from SV 40 large-T antigen was included as a positive control [14], and the results showed that none of the IMP1 segments was capable of mediating import in NIH 3T3 cells.

An RNA-binding mutant protein with increased nuclear entry

Since the ability of IMP1 to bind RNA is a prerequisite for the formation of granules with an optical diameter of 200–700 nm [2], which probably was unable to enter the nucleus, we designed a full-length mutant IMP1 protein exhibiting a decreased RNA-binding affinity without jeopardizing the overall protein structure. We utilized the Nova-2 KH3–RNA co-crystal structure [18], which exhibits a salt bridge between the lysine residue at position 2 in the GXXG loop and the sugar-phosphate backbone, and substituted the lysine residues with glutamic residues in the

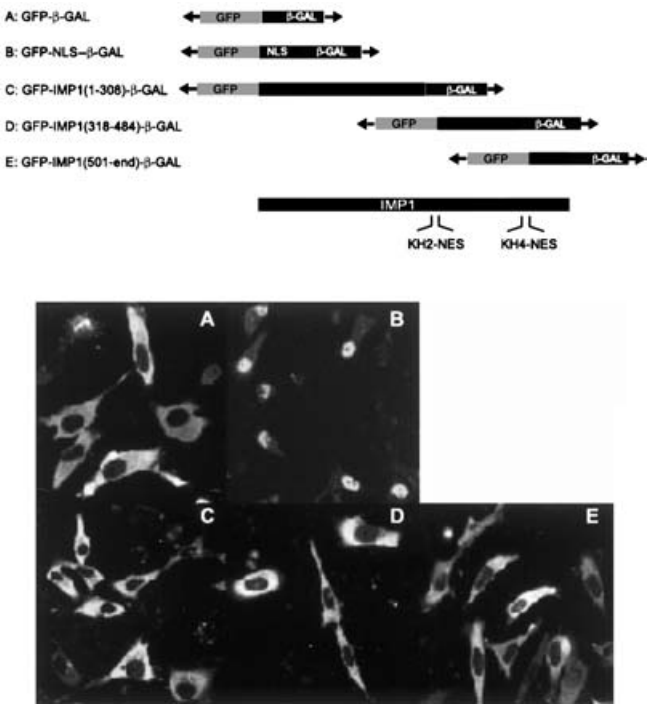

Figure 4 Import signal analysis

Truncated versions of IMP1 containing amino acids 1–308 (construct C), 318–484 (construct D) and 501–577 (construct E), without the two export signals (see legend to Figure 8), were fused in frame between GFP and β-galactosidase and transfected into NIH 3T3 cells. The parent plasmid (construct A) is pHM 830 [14], and the positive control (construct B) encompasses the NLS from SV 40 large-T antigen.

GXXG loops of KH1–KH3 domains in the full-length IMP1 context. The resulting mutant GFP–IMP1(GXXG) protein was present in the nucleus in >80% of the cells (Figure 5A). Moreover, the characteristic cytoplasmic granular appearance of the wild-type protein was abolished. Nuclear translocation as revealed by an FRAP analysis showed that half-maximal recovery occurred within 3 min (Figure 5C). In contrast, the GFP–luciferase control protein which exhibits a similar molecular mass of 90 kDa, was unable to enter the nucleus within 40 min. Hence we infer that the mutant GFP–IMP1(GXXG) protein, where XX in the signature loop of KH1–KH3 domains contains EL, exhibits decreased RNA-binding affinity (Figure 5B) and cannot participate in cytoplasmic granule formation, thereby giving rise to an increased pool of free protein that rapidly enters the nucleus.

IMP1 contains two NESs within its RNA-binding modules

To identify the NESs in IMP1, a series of deletion mutants were fused to GFP and transfected into NIH 3T3 cells (Figure 6). All the constructs encoded proteins smaller than the 50 kDa diffusion limit of the nuclear pores, so that, in the absence of transport signals, an equal distribution between the nucleus and the cytoplasm was anticipated. The fusion proteins that contained the second or the fourth KH domain from IMP1 (designated KH2 and KH4) accumulated in the cytoplasm, whereas all other constructs were distributed equally between the two compartments. Further deletion of KH2 and KH4 led to the identification of NESs within the KH domains (Figure 6).

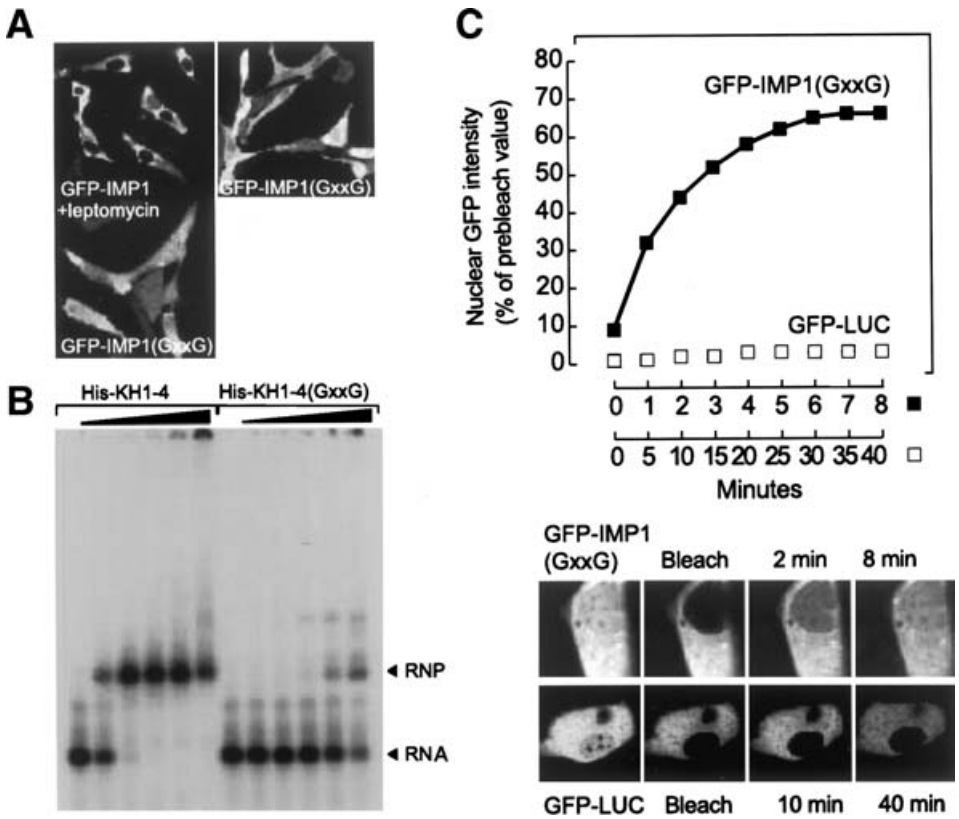

Figure 5 Analysis of the mutant GFP–IMP1(GXXG) protein

(**A**) NIH 3T3 cells transiently transfected with GFP–IMP1 (1), GFP–IMP1(GXXG) (2) or GFP–IMP1(GXXG) in the presence of 2 nM leptomycin B (3). (**B**) Electrophoretic mobility-shift analysis of a reduced SELEX target (nt 781–866 in the mouse IGF-II 3′-UTR) with recombinant wild-type KH1-4 and mutant KH1-4(GXXG) proteins. The His–KH1-4(GXXG) mutant was obtained by inserting EL for XX into the signature loops of the KH1, KH2 and KH3 domains. Lanes 1 and 7, 0 nM; lanes 2 and 8, 0.3 nM; lanes 3 and 9, 1 nM; lanes 4 and 10, 3 nM; lanes 5 and 11, 10 nM; lanes 6 and 12, 30 nM. (**C**) FRAP analysis of the nuclear staining of GFP–IMP1(GXXG) mutant protein and the similarly sized GFP–firefly luciferase. Western-blot analysis of transfected cells could not detect proteolysis of the mutant GFP–IMP1(GXXG) protein (results not shown).

NES in KH2

In KH2, a 12-amino-acid peptide was found to be sufficient to mediate cytoplasmic accumulation of a GFP-fusion protein in 80–90 % of the cells. This peptide exhibited close similarity to the leucine-rich NES in Rev (Figure 7A), and GFP–KH2 in which L318 (Leu^{318}) and L320 were changed to alanine residues were not exported (results not shown). Moreover, the export mediated by KH2 could be blocked by leptomycin B (Figure 8A), indicating that it is mediated by the CRM1 export pathway.

The structure of one of the KH domains from the splicing factor Nova-2 had been determined both alone and in complex with RNA [18,19]. Threading of KH2 over this structure revealed that the NES in KH2 was situated in the variable loop between β-strands 2 and 3 (Figure 7B).

NES in KH4

Whereas leptomycin B treatment blocked the export mediated by the NES in KH2, and had a partial effect on the full-length GFP–IMP1(GXXG) mutant protein, both full-length ‘wild-type’ GFP–IMP1 and GFP–KH4 were unaffected in NIH 3T3 cells. This indicated that the KH2–NES might be redundant in the full-length protein and that KH4 mediates export by an alternative pathway (Figure 8A). To substantiate that the two NESs operated via distinct pathways within the same cell, KH2 and KH4 NESs were fused to CFP and YFP (cyan and yellow fluorescent protein) respectively, and co-transfected into NIH 3T3 cells. Corresponding to the higher export fraction of KH2, more cells exhibited export of CFP–KH2 compared with those of YFP–KH4. However, in a smaller fraction, export of YFP–KH4 but not of CFP–KH2 was apparent (Figure 8B).

To verify that the observed KH4-mediated cytoplasmic accumulation was due to export and not due to cytoplasmic retention, an FRAP analysis was performed in cells transfected with GFP fused to the NES in KH4. Figure 9(A) illustrates that GFP–KH4 in the nucleus and the cytoplasm equilibrates within minutes after bleaching the nucleus, indicating that GFP–KH4 is not retained in the cytoplasm.

Moreover, we fused GFP–KH4 to TCP-80/NF90, which contains a strong bipartite and lysine-rich NLS [20]. Figure 9(B) shows that the NES in KH4 is capable of overriding the NLS in TCP-80/NF90, but nucleolar TCP80/NF90 is unaffected.

To define the KH4 export signal, we examined a series of GFP–KH4 deletion constructs. The analysis revealed that 11 residues from KH4 were sufficient to mediate export, but the entire KH4 was needed for full export activity (Figure 9C). The N-terminus of the NES in KH4 was sharply defined by E485, the deletion of which abolished the activity completely, whereas the C-terminus of the NES was not well defined. The N-terminal residues 485–527 retained almost full activity with distinct cytoplasmic accumulation in approx. 30 % of the cells (compared with approx.

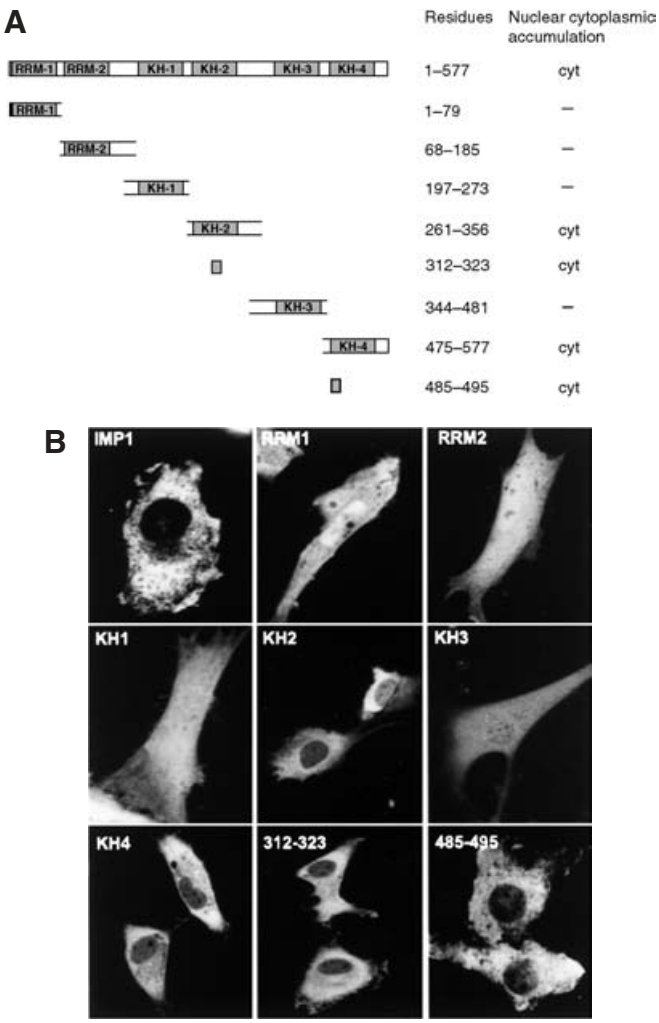

Figure 6 Identification of NESs in IMP1 by deletion analysis

Overlapping segments of human IMP1 each containing one putative RNA-binding module was fused to GFP and transiently transfected into NIH 3T3 cells. (**A**) Schematic overview of constructs and their cytoplasmic/nuclear accumulation (– indicates an equal distribution). (**B**) Representative pictures of each construct after transient transfection.

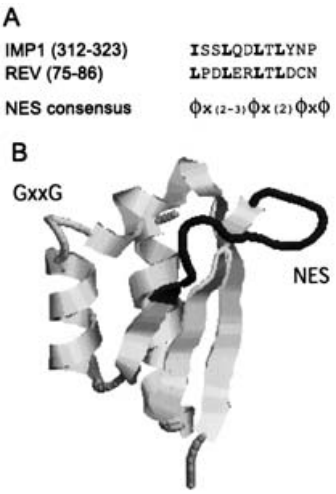

Figure 7 Characterization of the NES in KH2

(**A**) Alignment of the NES in KH2 with the NES from the HIV-1 Rev protein. Identical or similar positions of hydrophobic residues are shown in boldface. A 'leucine-rich' NES consensus derived from strong export signals is shown below; most leucine residues can be substituted by hydrophobic amino acids (Φ) without loss of activity [30,31]. (**B**) Threading of IMP1 KH2 over the crystallized KH domain from Nova-2 KH3 [18]. The NES in KH2 and the GXXG loop are indicated. Threading was performed with the Modeller4 program [32].

40 % for full-length KH4), whereas smaller constructs exhibited decreased export activity. The smallest peptide that conferred some export activity consisted of residues 485–495. Threading of KH4 over the Nova-2 KH domain structure showed that the core of the KH4 NES encompassed two amino acids in the presumed flexible region immediate to the N-terminus of the KH domain and the first β-strand (see Figure 7B). To identify critical residues, the core region was subjected to site-directed mutagenesis (Figure 9D). Three of the ten tested amino acid substitutions (V486A, L488A and I492A) abolished export activity completely, whereas a few others decreased export activity substantially. Thus KH4 NES had one charged residue (E485) and three hydrophobic residues that were essential for activity, and at least six others that enhanced the activity.

To establish that the NES in KH4 functions in the full-length context of GFP–IMP1, the following mutations were constructed and examined: V486A, EE484–485AL, EEV484–486AAA, VKL486–488AAA and HIR491–493AAA. None of the mutations caused a major shift in the subcellular localization of the protein, and varying degrees of granule formation and cytoplasmic aggregation (results not shown) made inferences regarding nuclear entry difficult.

The NES in KH4 is conserved in the recently identified IMP1 *Drosophila* homologue, dIMP [3]. Fusion of the *Drosophila* KH4 module to GFP resulted in the export of the tagged module in mouse NIH 3T3 cells with an efficiency similar to KH4 from human IMP1. Comparison of the human and *Drosophila* KH4 domains (Figure 9D) revealed that the identified critical E485, V486, L488 and I492 residues in the human protein were conserved with either identical or similar amino acids at the equivalent positions in the *Drosophila* protein. In conclusion, KH4 contained a conserved NES with critical charge and hydrophobic residues, which function through a leptomycin B-insensitive pathway.

DISCUSSION

IMP1 belongs to a conserved family of RBPs that participate in cytoplasmic processes such as mRNA localization, turnover and translational control. In the present study, we demonstrate that IMP1 is capable of translocating into the nucleus *in vivo* and contains two NESs, situated within the second and fourth KH modules.

The nuclear transit of GFP–IMP1 is relatively fast. On the basis of the FRAP analysis, we estimated that 50 % of a nuclear GFP–IMP1 population is recovered within 25 min. This is decreased to 3 min when the mutant GFP–IMP1(GXXG) protein, that cannot form granules, is used. In comparison, the well-characterized hnRNP A1 shuttling protein uses 6 h in a heterokaryon assay [21]. The nuclear accumulation of wild-type protein is mainly observed in cultured cells, expressing relatively high levels of IMP1. A plausible explanation is that these cells exhibit an increased pool of free IMP1 due to saturation of RNA targets, a conclusion reinforced by the behaviour of the RNA-binding mutant. In agreement with recent results [9], it is likely that IMP1 is loaded with its target RNA in the nucleus and becomes exported as an RNP. In fact, nuclear GFP–IMP1 exhibits a very

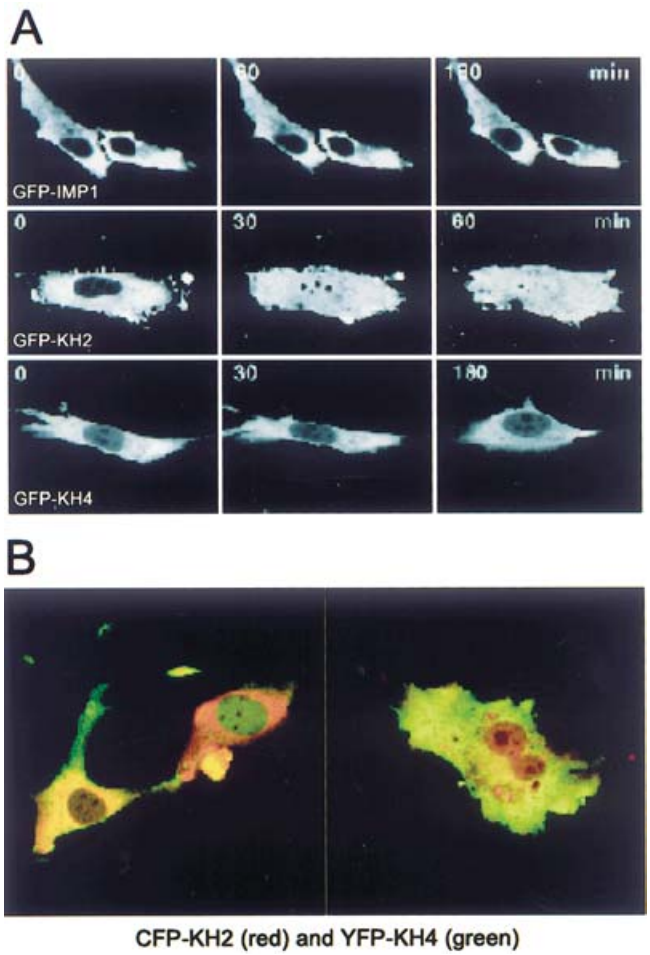

Figure 8 The two NESs utilize independent export pathways

(**A**) The export of KH2, but not KH4 and full-length IMP1, is sensitive to leptomycin B treatment. NIH 3T3 cells stably expressing GFP–IMP1 or NIH 3T3 cells transiently transfected with GFP–IMP1 [310–324] (GFP–KH2) or GFP–IMP1 [485–513] (GFP–KH4) were exposed to 2 nM leptomycin B, after which the cells were followed by time-lapse microscopy. All cells transfected with GFP–KH2 exhibited equal distribution of staining between the nucleus and the cytoplasm after exposure to leptomycin B for 1 h. There was no effect on the distribution in cells expressing GFP–IMP1 or GFP–KH4. (**B**) CFP–KH2 and YFP–KH4 (displayed in red and green pseudo-colours respectively to aid visualization) were co-transfected into NIH 3T3 cells to reveal their independent transport behaviour.

low diffusion rate, implying an association with macromolecular components in the nucleus (F. C. Nielsen, J. Nielsen, S. K. Adolph and J. Christiansen, unpublished work). Yeast She2p that shuttles between the cytoplasm and the nucleus is also exported in an RNA-dependent manner [22]. Moreover, the requirement for RNA-binding activity for cytoplasmic retention and localization may be a more general theme since it has been observed with the MSY2 protein, which is a mouse germ-cell-specific Y-box protein implicated in global regulation of stability and/or translation of maternal oocyte mRNAs [23].

A major concern was to identify an organ reflecting the cell-culture observations. Therefore the finding of IMP1 immunoreactivity in nuclei of spermatogenic cells indicated that nuclear import also took place in the intact organism. Nuclear entry may not be restricted to testis, since *Xenopus* pancreatic islet cells also appeared to exhibit exclusive nuclear staining (R. Stein, personal communication). Furthermore, Vg1 RNA-binding protein immunoreactivity was apparent in the germinal vesicle of stage I oocytes [24], IMP3 appeared to be a component of the spliceosome in HeLa cells [8] and chicken ZBP1 had been imaged to nuclear pre-mRNAs [9]. So far the mechanism of import is unclear. We have not been able to pinpoint a simple NLS, which may indicate that import involved a complex protein interaction or that the import signal overlapped one of the export signals, as previously found for the M9 signal in hnRNP A1 [21] and the KNS signal in hnRNP K [25]. Since the mutant IMP1(GXXG) protein enters, but does not appear to accumulate in the nucleus, facilitated diffusion may be a probable mechanism of entry.

The deletion analysis revealed two putative NESs in IMP1. The first leptomycin B-sensitive NES in KH2 is situated in the variable loop in the vicinity of the RNA attachment site reported for Nova [18]. The export sequence is similar to the leucine-rich NES in Rev, and in the context of the isolated KH2 domain the signal mediates an efficient export. The subcellular distribution of the full-length IMP1 molecule was insensitive to leptomycin B, at least in the present experimental system, but the IMP1(GXXG) mutant exhibited partial sensitivity towards leptomycin B. This difference is a probable consequence of the increased flux of mutant protein into the nucleus, giving rise to a shift in the steady-state balance between the two compartments. Moreover, the KH2–NES in the mutant protein may be more accessible to CRM1, since it is not engaged in RNA binding.

The core of the NES in KH4 consists of two N-terminal amino acids of the KH domain and the first β-strand. So, this NES is probably optimized to function in its natural structural context. This may explain the lower export activity observed with the unstructured GFP peptides from the KH4 domain. Therefore it is possible that the NES is only composed of the core (residues 485–495) and that the enhancing effect of the remaining KH domain merely reflects an optimal display of the NES. Four residues are absolutely required for the function of the KH4–NES: the hydrophilic residue E485 and three hydrophobic residues V486, L488 and I492. The relatively conservative substitution of these large hydrophobic side-chains with the smaller hydrophobic alanine side-chain leads to a loss of export activity, suggesting that these residues could be directly involved in the interaction with the export machinery. Apart from the CRM1 export pathway, it is only the calreticulin export pathway that has been reported to depend on hydrophobic residues [26]. The NES in KH4 is phylogenetically conserved in the *Drosophila* homologue of IMP1, whereas sequence comparison suggests that this is not the case for the NES in KH2. Both the function and the macromolecular interaction of the KH4–NES thus appear to be conserved through evolution, suggesting that it is important for the function of IMP. Several mutations in the KH4–NES in the full-length molecule led to protein aggregates in the cytoplasm, emphasizing the importance of the structural integrity of the first β-strand in KH4 in the context of the full-length protein.

IMP1 is unusual in several aspects. First, IMP1 is not ubiquitously expressed *in vivo* but reveals a restricted spatio-temporal expression. Secondly, IMP1 interacts with a subset of mRNA targets. Finally, IMP1 is mainly cytoplasmic at steady state. FMRP is the only other RBP reported to exhibit similar features [27]. The IMP proteins are expressed during the early stages of embryogenesis and at a burst at embryonic day 12.5 in the mouse. The sharp increase in IMP1 may define the cytoplasmic fates of a subset of mRNAs, including IGF-II, H19, c-*myc* and β-actin RNAs, which all play essential roles in the growth and migration of cells during development. As recently proposed, the nuclear entry of IMP1 indicates that the protein may attach to its RNA targets and thereby define the cytoplasmic fate of the transcripts in terms of granule formation, localization, stability and translatability shortly after transcription [28,29].

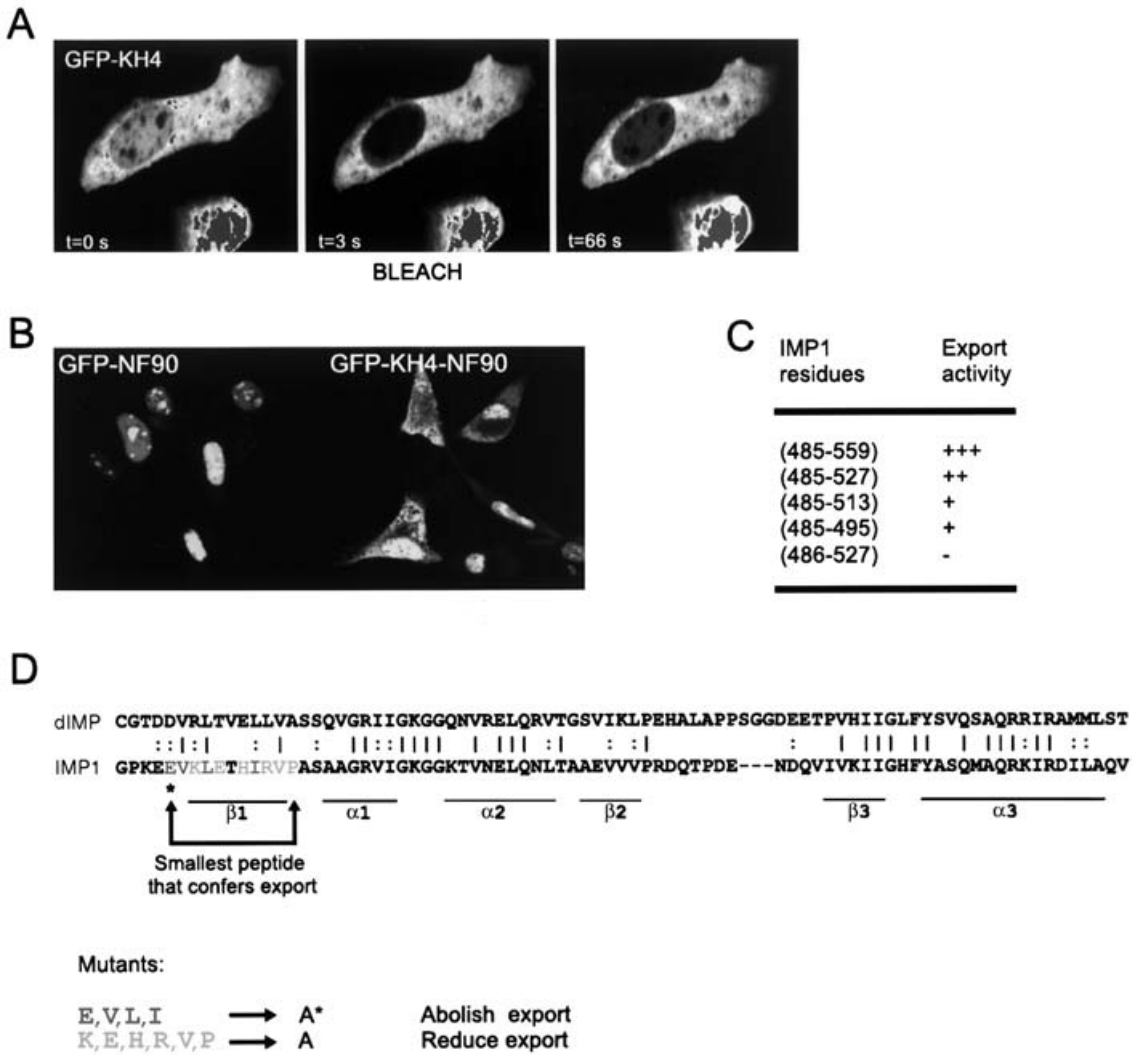

Figure 9 Characterization of the NES in KH4

(**A**) FRAP experiment showing that cytoplasmic accumulation of GFP–KH4 is due to export and not due to cytoplasmic retention. The nuclear fluorescence was bleached and recovery was seen after 1 min. (**B**) NIH 3T3 cells transiently transfected with GFP–NF90 and GFP–KH4–NF90. (**C**) Deletion analysis of KH4 from human IMP1. The export activity of the indicated GFP-fusion constructs was evaluated by counting the number of cells that exhibit distinct export (essentially black nuclei) of fusion protein. Representative percentages were 40 % for full-length KH4, 30 % for 485–527, 10–15 % for 485–513 and 10–15 % for 485–495. (**D**) Analysis of the NES in KH4 by site-directed mutagenesis and phylogenetic comparison. The KH4 domains with flanking residues from the *Drosophila* homologue dIMP and the human IMP1 are aligned with identical residues marked by '|' and similar residues by ':'. The predicted secondary structural elements of the KH domain are underlined; compare with the KH-fold in Figure 7(B). The arrowed bracket indicates the smallest segment (485–495) that is capable of conferring export. The significance of the individual residues within the 485–495 segment for NES activity was examined by alanine substitution mutagenesis of the GFP–IMP1[485–527] construct. Residues that abolished export after mutation are marked in dark grey, and residues that decreased export significantly are marked in light grey. Residues marked in black have not been tested by mutation. *Significance of E485 was not shown by site-directed mutagenesis, but by deletion analysis.

We are grateful to Thomas Stamminger (Institut für Klinische und Molekulare Virologie der Universität Erlangen-Nürnberg, D-91054 Erlangen, Germany) for the pHM series of plasmids. We also thank Lena B. Johansson and Joan Christiansen for their excellent technical assistance. The research was supported by the Danish Natural Science and Medical Research Councils, the Novo Nordisk Foundation, the Danish Cancer Society and the Toyota Foundation.

REFERENCES

1 Yaniv, K. and Yisraeli, J. K. (2002) The involvement of a conserved family of RNA binding proteins in embryonic development and carcinogenesis. Gene **287**, 49–54
2 Nielsen, F. C., Nielsen, J., Kristensen, M. A., Koch, G. and Christiansen, J. (2002) Cytoplasmic trafficking of IGF-II mRNA-binding protein by conserved KH domains. J. Cell Sci. **115**, 2087–2097
3 Nielsen, J., Cilius Nielsen, F. C., Kragh Jakobsen, R. and Christiansen, J. (2000) The biphasic expression of IMP/Vg1-RBP is conserved between vertebrates and *Drosophila*. Mech. Dev. **96**, 129–132
4 Nielsen, J., Christiansen, J., Lykke-Andersen, J., Johnsen, A. H., Wewer, U. M. and Nielsen, F. C. (1999) A family of insulin-like growth factor II mRNA-binding proteins represses translation in late development. Mol. Cell. Biol. **19**, 1262–1270
5 Nielsen, F. C., Nielsen, J. and Christiansen, J. (2001) A family of IGF-II mRNA binding proteins (IMP) involved in RNA trafficking. Scand. J. Clin. Lab. Invest. Suppl. **234**, 93–99
6 Doyle, G. A., Betz, N. A., Leeds, P. F., Fleisig, A. J., Prokipcak, R. D. and Ross, J. (1998) The c-*myc* coding region determinant-binding protein: a member of a family of KH domain RNA-binding proteins. Nucleic Acids Res. **26**, 5036–5044
7 Zhang, H. L., Eom, T., Oleynikov, Y., Shenoy, S. M., Liebelt, D. A., Dictenberg, J. B., Singer, R. H. and Bassell, G. J. (2001) Neurotrophin-induced transport of a β-actin mRNP complex increases β-actin levels and stimulates growth cone motility. Neuron **31**, 261–275

8 Zhou, Z., Licklider, L. J., Gygi, S. P. and Reed, R. (2002) Comprehensive proteomic analysis of the human spliceosome. Nature (London) **419**, 182–185
9 Oleynikov, Y. and Singer, R. H. (2003) Real-time visualization of ZBP1 association with β-actin mRNA during transcription and localization. Curr. Biol. **13**, 199–207
10 Gorlich, D. and Kutay, U. (1999) Transport between the cell nucleus and the cytoplasm. Annu. Rev. Cell Dev. Biol. **15**, 607–660
11 Nakielny, S. and Dreyfuss, G. (1999) Transport of proteins and RNAs in and out of the nucleus. Cell (Cambridge, Mass.) **99**, 677–690
12 Krecic, A. M. and Swanson, M. S. (1999) hnRNP complexes: composition, structure, and function. Curr. Opin. Cell Biol. **11**, 363–371
13 Morgenstern, J. P. and Land, H. (1990) Advanced mammalian gene transfer: high titre retroviral vectors with multiple drug selection markers and a complementary helper-free packaging cell line. Nucleic Acids Res. **18**, 3587–3596
14 Sorg, G. and Stamminger, T. (1999) Mapping of nuclear localization signals by simultaneous fusion to green fluorescent protein and to β-galactosidase. BioTechniques **26**, 858–862
15 Fu, L., Suen, C. K. M., Waseem, A. and White, K. N. (1997) Variable requirement for splicing signals for nucleocytoplasmic export of mRNAs. Biochem. Mol. Biol. Int. **42**, 329–337
16 Singer, B. S., Shtatland, T., Brown, D. and Gold, L. (1997) Libraries for genomic SELEX. Nucleic Acids Res. **25**, 781–786
17 Rajpert-De Meyts, E., Jorgensen, N., Graem, N., Muller, J., Cate, R. L. and Skakkebaek, N. E. (1999) Expression of anti-Mullerian hormone during normal and pathological gonadal development: association with differentiation of Sertoli and granulosa cells. J. Clin. Endocrinol. Metab. **84**, 3836–3844
18 Lewis, H. A., Musunuru, K., Jensen, K. B., Edo, C., Chen, H., Darnell, R. B. and Burley, S. K. (2000) Sequence-specific RNA binding by a Nova KH domain: implications for paraneoplastic disease and the fragile X syndrome. Cell (Cambridge, Mass.) **100**, 323–332
19 Lewis, H. A., Chen, H., Edo, C., Buckanovich, R. J., Yang, Y. Y., Musunuru, K., Zhong, R., Darnell, R. B. and Burley, S. K. (1999) Crystal structures of Nova-1 and Nova-2 K-homology RNA-binding domains. Structure Fold. Des. **7**, 191–203
20 Reichman, T. W., Muniz, L. C. and Mathews, M. B. (2002) The RNA binding protein nuclear factor 90 functions as both a positive and negative regulator of gene expression in mammalian cells. Mol. Cell. Biol. **22**, 343–356
21 Michael, W. M., Siomi, H., Choi, M., Pinol-Roma, S., Nakielny, S., Liu, Q. and Dreyfuss, G. (1995) Signal sequences that target nuclear import and nuclear export of pre-mRNA-binding proteins. Cold Spring Harb. Symp. Quant. Biol. **60**, 663–668
22 Kruse, C., Jaedicke, A., Beaudouin, J., Bohl, F., Ferring, D., Guttler, T., Ellenberg, J. and Jansen, R. P. (2002) Ribonucleoprotein-dependent localization of the yeast class V myosin Myo4p. J. Cell Biol. **159**, 971–982
23 Yu, J., Hecht, N. B. and Schultz, R. M. (2003) Requirement for RNA-binding activity of MSY2 for cytoplasmic localization and retention in mouse oocytes. Dev. Biol. **255**, 249–262
24 Zhang, Q., Yaniv, K., Oberman, F., Wolke, U., Git, A., Fromer, M., Taylor, W. L., Meyer, D., Standart, N., Raz, E. et al. (1999) Vg1 RBP intracellular distribution and evolutionarily conserved expression at multiple stages during development. Mech. Dev. **88**, 101–106
25 Michael, W. M., Eder, P. S. and Dreyfuss, G. (1997) The K nuclear shuttling domain: a novel signal for nuclear import and nuclear export in the hnRNP K protein. EMBO J. **16**, 3587–3598
26 Holaska, J. M., Black, B. E., Love, D. C., Hanover, J. A., Leszyk, J. and Paschal, B. M. (2001) Calreticulin is a receptor for nuclear export. J. Cell Biol. **152**, 127–140
27 Bardoni, B. and Mandel, J. L. (2002) Advances in understanding of fragile X pathogenesis and FMRP function, and in identification of X linked mental retardation genes. Curr. Opin. Genet. Dev. **12**, 284–293
28 Dreyfuss, G., Kim, V. N. and Kataoka, N. (2002) Messenger-RNA-binding proteins and the messages they carry. Nat. Rev. Mol. Cell Biol. **3**, 195–205
29 Farina, K. L. and Singer, R. H. (2002) The nuclear connection in RNA transport and localization. Trends Cell Biol. **12**, 466–472
30 Bogerd, H. P., Fridell, R. A., Benson, R. E., Hua, J. and Cullen, B. R. (1996) Protein sequence requirements for function of the human T-cell leukemia virus type 1 Rex nuclear export signal delineated by a novel *in vivo* randomization-selection assay. Mol. Cell. Biol. **16**, 4207–4214
31 Henderson, B. R. and Eleftheriou, A. (2000) A comparison of the activity, sequence specificity, and CRM1-dependence of different nuclear export signals. Exp. Cell Res. **256**, 213–224
32 Sali, A., Potterton, L., Yuan, F., van Vlijmen, H. and Karplus, M. (1995) Evaluation of comparative protein modeling by MODELLER. Proteins **23**, 318–326

Received 24 June 2003/4 August 2003; accepted 18 August 2003
Published as BJ Immediate Publication 18 August 2003, DOI 10.1042/BJ20030943